Adsorption of Ethyl Alcohol on Silica Gel

SHINOBU MASAMUNE and J. M. SMITH

University of California, Davis, California

This work utilizes the developments of the foregoing paper (*10*) to analyze adsorption data, in the form of breakthrough curves, for ethyl alcohol on silica gel at 90° to 155°C. It was found that for the smallest particle size, and in the lower part of the temperature range, the overall rate was determined by the surface adsorption process. At other conditions intraparticle diffusion was also a significant resistance in the overall process. The theoretical breakthrough curves agreed well with the experimental ones, so that the surface rate constant and diffusivity could be calculated.

Analysis of the diffusivity results showed that surface migration on the pore walls was the predominant contribution rather than gas-phase diffusion in the pore volume.

Suitable data are meager for evaluating the significance of reaction and diffusion steps in the overall adsorption process in porous solids. The equations presented in the preceding paper (*10*) indicate that measurements of adsorption rates on solid particles of different sizes are desirable in order to establish the importance of intraparticle diffusion. Similarly the resistance of the surface reaction step is best established with data taken over a temperature range. The published information on adsorption rates do not provide data on these two variables in general. Masamune and Smith (*9*) reported isothermal adsorption rates for nitrogen on Vycor porous glass over a range of particle sizes. Interpretation of these results indicated that intraparticle diffusion alone determined the rate for particle radii greater than 0.01 cm. Thus the physical adsorption step on the solid surface was of negligible resistance.

The objective of this report was to study experimentally a situation for which the surface adsorption resistance, as well as intraparticle diffusion resistance, was important in establishing the overall rate. For this purpose exit concentrations as a function of time were measured for the adsorption of ethyl alcohol from helium in beds of silica gel. Measurements were made at temperatures from 90.5° to 155°C. with gel particles whose radii covered the range 0.0099 to 0.0793 cm. With these small particles external diffusion resistance was negligible. Hence the equations in special cases 1 and 5 of Table 1 of the preceding paper were applicable for separating and evaluating intraparticle and surface adsorption resistances.

APPARATUS

A sorptometer (*1, 9*) was used for both the equilibrium and rate studies of the adsorption process. Figure 1 is a flow diagram of the apparatus. The helium (99.99 wt. % purity) entering the apparatus was separated at point *D*. The two streams were maintained at the desired constant flow rates by automatic pressure control valves (3) and lengths of restricted-diameter tubing (4). The flow rates were individually measured with especially accurate rotameters (5). Before entering the flow rate control system the small amount of residual water in the helium was removed by a bed of silica gel (2). An equilibrium ethyl alcohol-helium mixture was obtained by introducing one stream into the helium-saturated bath of ethyl alcohol, maintained at 0°C. (6). To ensure equilibrium the contact efficiency between ethyl alcohol and helium was increased by dispersing the helium into small bubbles through a glass filter. The two streams were mixed again at point *J*. By adjusting the relative flow rates of two streams it was possible to vary the alcohol content of the combined streams from 0.00064 to 0.0161 mole fraction ethanol. The prepared gas mixture flowed to the reference side of the detector (7). This device consisted of a four filament (tungsten) thermal conductivity cell of the straight up, convection type in a bridge circuit. The entire cell was contained in a constant-temperature water bath. Leaving the cell the mixture entered a preheater bed consisting of a 10 cm. length of lead shot (100-μ diameter) (8) and then flowed directly into the sample bed of silica gel. Both beds were contained in Pyrex glass tubing, whose inside diameter was 0.476 cm. (cross-sectional area 0.178 sq. cm.). The entire Pyrex glass assembly (8) was maintained at the adsorption temperature by a surrounding electric heater. Temperature control within $\pm$ 1°C. was achieved by hand regulation. The temperature at the entrance of bed (bottom) was measured with a chromel-alumel thermocouple in a thermowell inserted in the Pyrex glass tubing as shown in Figure 1. The uniformity of the temperature profile along the axial direction of the bed was determined to be within $\pm$ 1.5°C. by measuring the temperatures at the entrance and exit of the bed for a limited number of runs. From the bed the gas entered the sensing side (10) of the detector and then was discharged through a soap-film meter (11).

The concentration difference of ethanol in the streams entering and leaving the bed was obtained by recording the exit readings from the detector.

A potential error in this work is due to dispersion of ethyl alcohol in the tubing between detector and exit of sample bed. This problem was investigated in an earlier paper (*9*). The results show that the concentration change due to this dispersion is negligible at the flow rate employed. No dehydration of alcohol was observed in the analysis of gases leaving the reactor.

OPERATING PROCEDURE

Before initiation of a run residual ethyl alcohol from the preceding run was completely desorbed by purging the preheater and sample beds with pure helium at 150°C. for about 2 hr. Then the system conditions, such as the flow rates and bath and adsorption temperatures, were set at desired values. Adsorption was initiated by introducing the one helium stream into the ethyl alcohol bath by use of glass cocks (*13*). This instant was taken as time $\theta = 0$, and the concentration change at the end of bed was recorded as a function of time. The time required to reach equilibrium in the entire bed was between 5 and 60 min. In analyzing the data correction was made for the holdup time between the bath and bed entrance as well as between the bed exit and the detector. The former was 20 sec. and the latter 12 sec., as determined experimentally at the operating velocity of 8.30 cm./sec. The run was terminated after the exit concentration again attained the feed concentration. This means that the adsorbed molecules in the bed are in equilibrium with the feed concentration throughout the bed, and no more adsorption occurs.

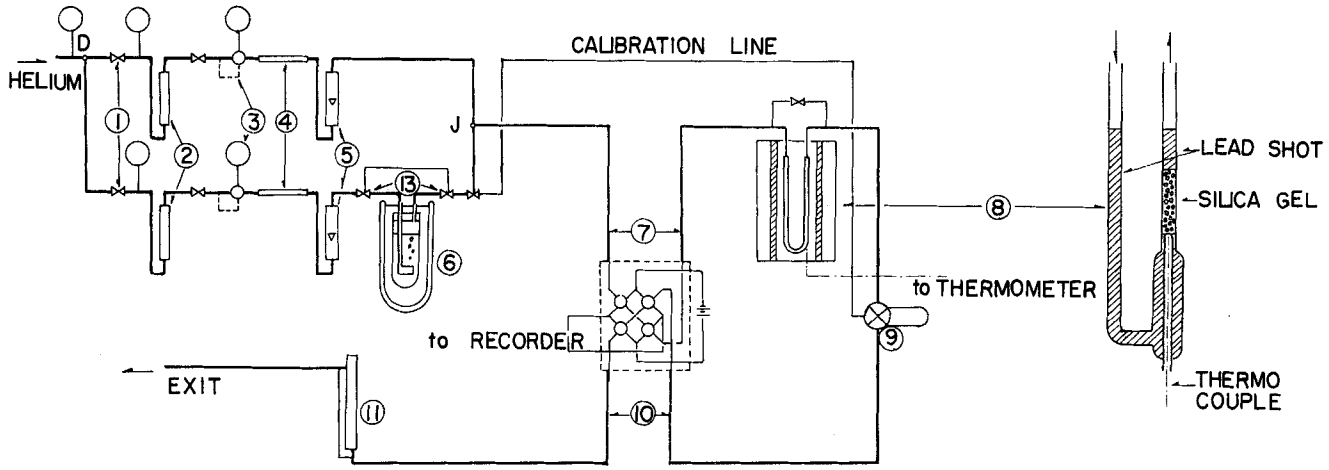

Fig. 1. Schematic drawing of adsorption apparatus.

Generally the recorded electromotive force curves are S-shaped, with time as abscissa and electromotive force as the ordinate. Illustrative curves are given in Figure 2, where the ordinate has been converted to $\bar{C}/\bar{C}_o$. The data cover two particle sizes $R = 0.0540$ and 0.0099 cm. at four different temperatures, 155°, 131°, 110°, and 90.5°C., for a constant bed length of 2.25 cm. The area bounded by $t = 0$, $\bar{C}/\bar{C}_o = 1$, and the breakthrough curves represents the maximum adsorption capacity of the bed for the inlet concentration $\bar{C}_o$. The shape of the curves is related to rates of adsorption. Analysis of this is the main objective of this paper.

PROPERTIES OF SILICA GEL AND EQUILIBRIUM DATA FOR ETHYL ALCOHOL

The physical properties of the silica gel used (SiO_2 = 99.71%) are shown in Table 1.

The equilibrium adsorption curve plotted as the amount of ethyl alcohol S_∞ against mole fraction P_e/P_h is illustrated in Figure 3 for $t = 110$°C. The figure indicates that the curve is linear up to P_e/P_h of 0.0020. On the same figure the coordinate on the right side shows the fraction θ_s of the total surface occupied by adsorbed molecules. This result is based upon 23Å^2 as the surface area for adsorption of one ethyl alcohol molecule (4). It is noted that a linear equilibrium curve holds until about 8% of the surface area is covered by adsorbed molecules.

In Figure 4 the isobaric equilibrium data at different temperatures (66.5° to 178°C.) but at constant ethyl alcohol concentration ($P_e/P_h = 0.00133$) are given. Here the equilibrium constant λ_e and θ_s are plotted vs. $1/T$. On the basis of the data in Figure 3 it is expected that the equilibrium isotherm would be linear up to a surface coverage of about 8%. The deviation of the data from a straight line in Figure 4 at the lowest temperature (66.5°C.) is apparently caused by the higher value of θ_s. In view of these data the theory developed in the preceding paper, which supposes a linear isotherm [Equation (65)], will be assumed applicable for the analysis of the present alcohol data, except at temperatures approaching 66.5°C.

The dependence of λ_e on temperature establishes the heat of adsorption as 10.8 Kcal./mole. This magnitude will be discussed later.

SCOPE OF DATA

Silica gel (6 to 16 mesh) was fractured, ground, and separated into six fractions by conventional sieve analysis. The average particle radii studied as well as the range of other variables is given in Table 2.

QUALITATIVE ANALYSIS OF DATA

The time abscissa of the recorded curves, illustrated in Figure 2, were first transformed to the dimensionless time

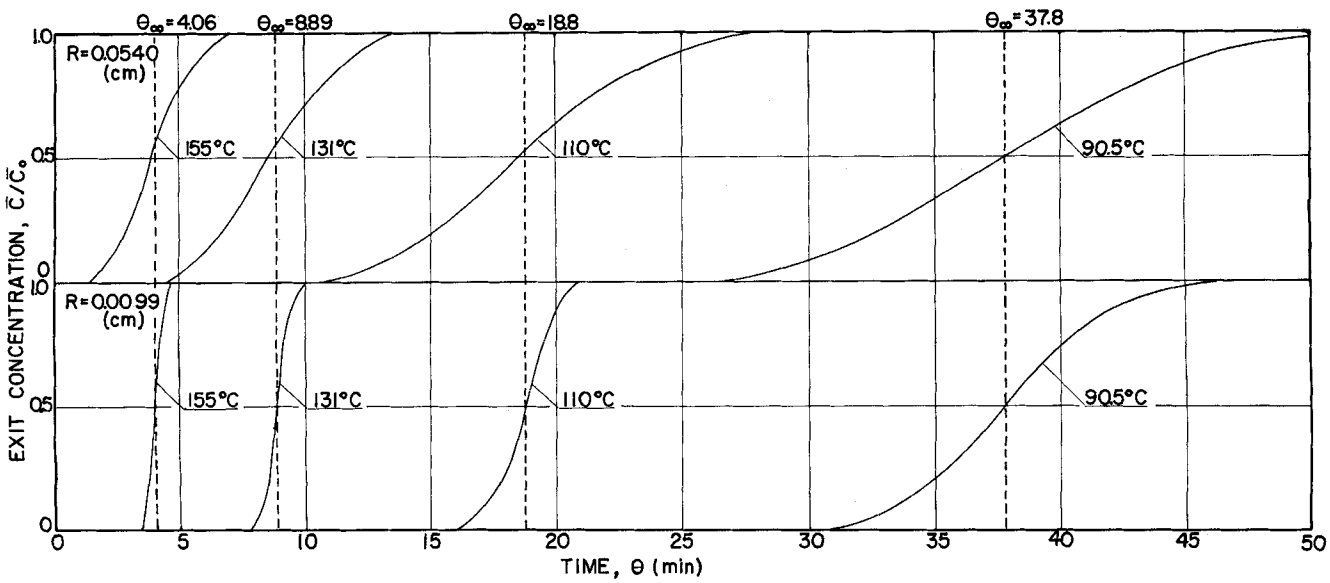

Fig. 2. Breakthrough curves for various temperatures.

TABLE 1

Surface area, $\overline{S}^*$	8.32×10^6 sq. cm./g.
Void volume, $\overline{V}^*$	0.43 cc./g.
Average pore radius, $\overline{r}^*$	11Å ($2\overline{V}/\overline{S}$)
Void fraction, ϵ_p	0.486
Particle density, ρ_p	1.13 g./cc.
True density, ρ_t (6)	2.20 g./cc.

TABLE 2

Average particle radius, R		0.0793, 0.0540, 0.0311, 0.0151, 0.0099 cm.
Temperature, T	For rate measurements	155°, 131°, 110°, 100°, and 90.5°C.
	For equilibrium measurements	178 to 66.5°C.
Flow rate, u		8.30 cm./sec. (0°C., 1 atm.)
Total pressure, p		Atmospheric
Bed length, z_o		2.25 cm.
Interparticle void fraction, ϵ_B		0.359
Bulk density of bed, ρ_B		0.748 g./cc.
Inlet ethyl alcohol concentration, $\overline{C}_o$		5.94×10^{-8} mole/cc.

parameter $\theta_o = \theta/\theta_\infty$. The points in Figures 5 and 6 show examples of these transformed data at the lowest (90.5°C.) and at the highest temperature (155°C). In each case the data cover the five particle sizes shown in Table 2. Examination of these curves and those for the intermediate temperatures indicate two effects with respect to particle size and temperature:

1. Effect of particle size. In each set of data at constant temperature particle size has a significant effect on the shape of the breakthrough curves. Generally the overall adsorption rate increases with decrease in particle size; that is the curves for the smaller particles becomes more vertical, approaching the infinite rate line at high temperatures.

2. Effect of temperature. The effect of particle size on the adsorption curves is strongly dependent on temperature. That is the particle size effect becomes less significant with a decrease in temperature. Experimentally no difference is observed between the two curves for the two smallest particles (R = 0.0099 and 0.0151 cm.) at temperatures of 90.5° and 100°C. This is shown at 90.5°C. in Figure 5 where the experimental data for the two smallest particles are seen to coincide. The theoretical development described in the preceding paper shows that the adsorption is strongly dependent upon particle size when intraparticle

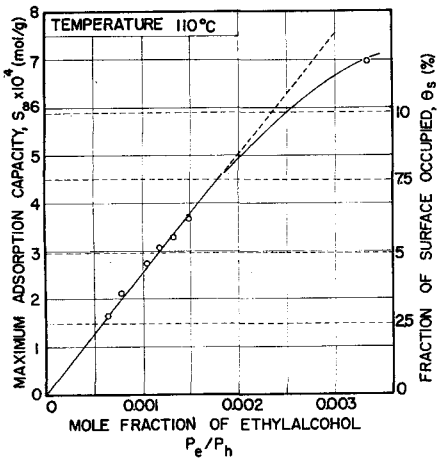

Fig. 3. Equilibrium adsorption curve at 110°C.

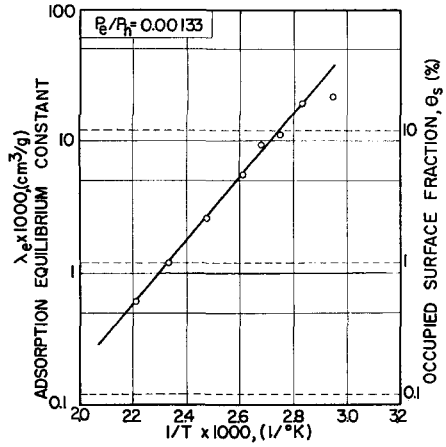

Fig. 4. Adsorption equilibrium constant as a function of temperature.

diffusion controls the rate and independent of particle size when surface adsorption controls the rate (Case 5). In addition when the activation energy for adsorption is significant, the temperature affects the adsorption rate constant much more strongly than the diffusion coefficient.

These considerations indicate that the observed adsorption curves in general represent the combined effect of two contributions, intraparticle diffusion resistance and surface adsorption rate resistance. [The possibility of external diffusion influencing the rate was tested in a previous study (9) for similar particle sizes and velocities. It was found that this resistance was negligible]. As one extreme case intraparticle diffusion should control the overall rate at a high temperature and for large particles, while at the other extreme the process is governed solely by surface adsorption rate at low temperatures and for small particles.

QUANTITATIVE ANALYSIS OF DATA

Equation (52) of the preceding paper describes the breakthrough curve when both intraparticle diffusion and surface adsorption are important resistances. Two unknown parameters, the surface rate constant $\vec{\lambda}$ and the diffusivity D_i, prevent immediate application of this expression to the data. However $\vec{\lambda}$ can be evaluated by first using the part of the experimental data where the overall rate is governed solely by the surface adsorption process. Then Equation (52) can be applied to the bulk of the data to establish the intraparticle diffusivity D_i. It may be noted that the alternate approach of first determining the diffusivity cannot be used in this case. This is because for none of the data does intraparticle diffusion appear to be solely responsible for establishing the overall rate.

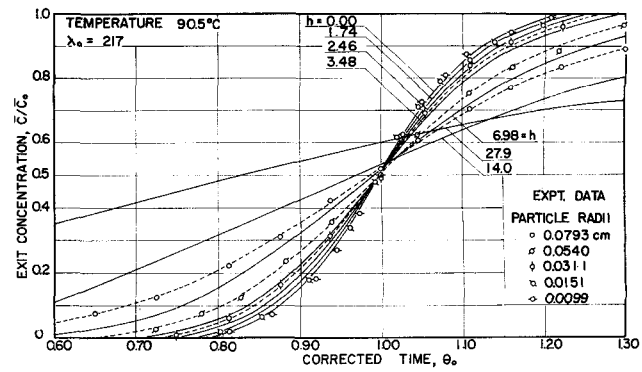

Fig. 5. Converted breakthrough curves at 90.5°C.

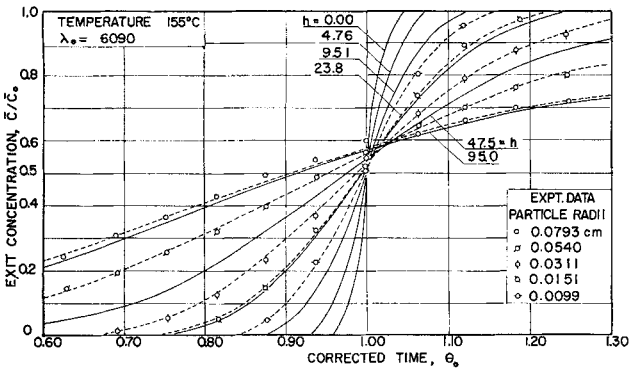

Fig. 6. Converted breakthrough curves at 155°C.

Evaluation of Adsorption (Surface) Rate Constant $\vec{\lambda}$

Since no size effect was observed for the two smallest particles (R = 0.0099 and 0.0151 cm.) at 90.5° and 100°C., these data should represent only the surface adsorption resistance. For 110°C. there was a small difference between the breakthrough curves for the two smallest particles. However extrapolation of the variation with particle size indicated that the curve for the smallest particle did not contain appreciable diffusion resistance. Hence the data for R = 0.0099 cm. at the three temperatures 90.5°, 100°, and 110°C. were used to compute $\vec{\lambda}$. The method was to plot first the theoretical breakthrough curves for this case for various values of λ_o. Such curves are shown in Figure 4 of the preceding paper (*10*). Next these theoretical curves were compared with the data to determine the best value of λ_o for each temperature. The results are:

t, °C.	λ_o
90.5	220
100	410
110	670

With these values of λ_o and Equation (49) of the preceding paper $\vec{\lambda}$ was evaluated, and the results are shown by the points at the three highest values of $1/T$ in Figure 7. These points, which form a straight line, establish the activation energy for surface adsorption. As a matter of interest the same procedure was usede to calculate a pseudo value of $\vec{\lambda}$ for temperatures of 131° and 155°C. even though intraparticle diffusion is an important resistance at these temperatures. The deviation between the extrapolated straight line and these pseudo points is due to this diffusion resistance.

The maximum observed in the curve in Figure 7 is worthy of comment. A lower rate of increase of rate constant than predicted from the Arrhenius straight line is commonly observed when gas-phase diffusion in catalyst pores becomes an important resistance. An actual decrease in rate constant as the temperature increases is less common. As described later this phenomenon gives an insight into the nature of the intraparticle diffusion process. The diffusivity must decrease rapidly with temperature for such a maximum in the Arrhenius plot to be observed. This indicates that the diffusion is primarily by migration of adsorbed molecules on the pore walls of the silica gel rather than the usual gas-phase diffusion in the pore volume.

The equation of the straight line in Figure 8 is

$$\vec{\lambda} = 2.57 \times 10^{11}\, e^{-13{,}700/RT} \text{ cc./(g. of adsorbate)(sec.)} \quad (69)$$

indicating an activation energy of 13,700 cal./g. mole. The rate constant $\vec{\lambda}'$ based upon the surface of the silica gel is obtained by dividing Equation (69) by the surface area, 832 sq. m./(g. of adsorbate). Hence

$$\vec{\lambda}' = 3.09 \times 10^{4}\, e^{-13{,}700/RT} \text{ cm./sec.} \quad (70)$$

Evaluation of Intraparticle Diffusivity

Equation (52) was employed first to calculate $\bar{C}/\bar{C}_o$ for various values of h (the diffusion parameter) at the constant values of λ_o determined from Equations (69) and (49) and the appropriate experimental temperatures. Examples of these calculated breakthrough curves at temperatures 90.5° and 155°C. are illustrated in Figures 5 and 6 by solid lines. As mentioned earlier the dotted lines and points represent experimental data. By superimposing the experimental and theoretical lines, optimum values of h were determined. Then the intraparticle diffusivity D_i was evaluated from Equation (36) and the known value of λ. This was done for each particle size and all the temperatures. The results are given in Table 3. While the procedure cannot be expected to lead to exact diffusivities, the similarity of values at a given temperature and varying particle size lends confidence to the anlaysis. The average values of D_i show a strong temperature dependency as shown on the upper Arrhenius line in Figure 8. The interpretation of these results is considered in the following section.

Pore and Surface Diffusion

The diffusivities shown in Table 3 represent the combined contribution (*2, 5*) of two-dimensional diffusion on the pore walls (surface diffusivity D_s) and gas-phase diffusion in the pore volume (pore diffusivity D_p). The pore diffusivity can be estimated from the random pore model of Wakao and Smith (*11*) and the porosity and mean pore radius of the silica gel given in Table 1. Since the pores in the gel are very small and the pressure atmospheric, pore diffusion is mainly by the Knudsen mechanism. The results of these calculations as a function of temperature are given by the lower line in Figure 8. The contribution of D_p to the total diffusivity D_i is seen to be less than 3%, even at the highest temperature. Therefore at the conditions of these experiments intraparticle diffusion is primarily of the surface type, and the D_i curve in Figure 8 can be considered to be an approximate measure of the surface diffusion rate.

Table 3. Intraparticle Diffusivities

Temp., °C.	90.5		100		110		131		155	
Particle radius, cm.	h	D_i, sq. cm./sec.	h	D_i, sq. cm./sec.	h	D_i, sq. cm./sec.	h	D_i, sq. cm./sec.	h	D_i, sq. cm./sec.
0.0793	8.5	0.11	15.5	0.075	27.0	0.032	50.1	0.027	97.0	0.023
0.0540	4.9	0.15			15.0	0.048	35.6	0.025	67.2	0.021
0.0311	3.0	0.14			9.5	0.040	17.0	0.035	35.6	0.025
0.0151					4.0	0.055	8.0	0.038	26.0	0.012
0.0099							2.0	0.026	14.5	0.016
Average		0.13		0.075		0.044		0.030		0.019

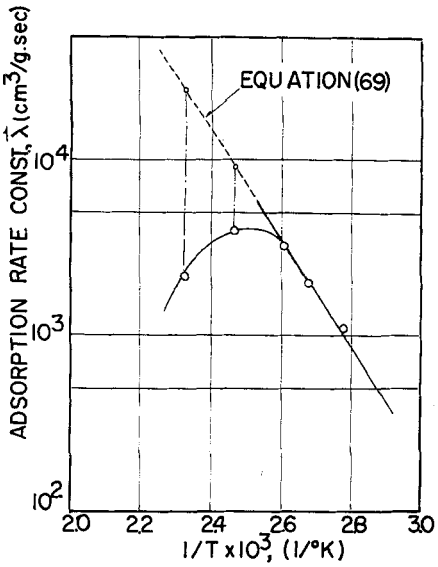

Fig. 7. Arrhenius plot for adsorption rate constant $\vec{\lambda}$.

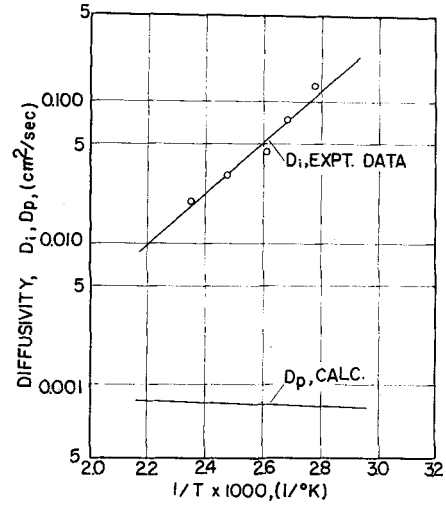

Fig. 8. Arrhenius plot for intraparticle diffusivity.

The sharp decrease in D_i with increasing temperature also suggests that surface diffusion is the predominant intraparticle transport process. This is because the fraction of the silica gel surface covered, and hence the opportunity for surface diffusion decreases with increasing temperature.

Type of Adsorption

In a recent review on chemisorption of alcohol on oxide catalysts such as silica gel and alumina Kipling et al. (7) reported that distinguishing between physical adsorption and chemisorption is very difficult. Particularly de Boer (3) suggested that the magnitude of the heat of adsorption is not always an adequate criterion because the expected heats of chemisorption and physical adsorption are nearly the same. Hence conclusive determination of the type of adsorption from the present data is not possible. However two points are of interest: the heat evolved on adsorption, from Figure 4, of 10.8 Kcal./mole is definitely higher than the heat evolved on condensation of pure alcohol, 9.40 kcal./mole, and the surface adsorption rate expressed by Equation (69) is very slow compared with usual rates of physical adsorption. For example the earlier work (9) on adsorption of nitrogen on Vycor glass at low temperature gave overall rates much higher than those found in this work [Equation (69)]. In fact for the nitrogen data the process was controlled by intraparticle diffusion, while for the present case the surface adsorption process controls the rate at the lower temperatures.

CONCLUSIONS

The results of this study indicate that the theory developed in the preceding paper saisfactorily explains the adsorption of ethyl alcohol on silica gel at low surface coverages. It was shown that at low temperatures and for the smallest particle size the overall rate was controlled by the surface reaction, while at higher temperatures both intraparticle diffusion and surface reaction resistances were significant.

Analysis of diffusivities calculated from the data indicate that surface migration along the pore walls is more important than gas-phase diffusion in the pores.

ACKNOWLEDGMENT

The financial assistance of the United States Army Research Office through Grant No. DA-ARO(D)-31-124-G191 is gratefully acknowledged.

NOTATION

In addition to that of preceding paper

D_p = pore diffusivity, sq. cm./sec.
D_s = surface diffusivity, sq. cm./sec.
P = total pressure, atm.
P_e = partial pressure of ethyl alcohol, atm.
P_h = partial pressure of helium, atm.
$\overline{r}$ = average pore radius of silica gel, A
$\overline{V}$ = void volume of silica gel, cc./g.
$\overline{S}$ = surface area of silica gel, sq. cm./g.
S_∞ = maximum (equilibrium) adsorption capacity of silica gel, g. mole alcohol/g.
R = particle radius, cm.

Greek Letters

$\vec{\lambda}'$ = adsorption rate constant based upon surface area, cm./sec.
θ_s = fraction of pore surface occupied by adsorbed ethyl alcohol

LITERATURE CITED

1. Ballow, E. V., and O. K. Doolen, *Anal. Chem.*, **32**, 532 (1960).
2. Barrer, R. M., and J. A. Barrie, *Proc. Roy. Soc.*, **A213**, 250 (1952).
3. de Boer, J. H., "Advances in Colloid Science," vol. 3, Interscience, New York and London (1950).
4. Emmett, P. H., "Catalysis," vol. 1, p. 37, Reinhold, New York (1954).
5. Glueckauf, E., and J. I. Coates, *J. Chem. Soc.*, 1315 (1947).
6. "Handbook of Chemistry and Physics," 30 ed., Chemical Rubber Publishing Co., Cleveland, Ohio (1947).
7. Kipling, J. J., and D. B. Peakall, "Chemisorption," p. 59, Butterworths Scientific Publications, London, England (1957).
8. Li, J. C. M., and P. Chang, *J. Chem. Phys.*, **23**, 518 (1955).
9. Masamune, Shinobu, and J. M. Smith, *A.I.Ch.E. Journal*, **10**, No. 2, p. 246 (1964).
10. *Ibid.*, **11**, No. 1, p. 34 (1965).
11. Wakao, N., and J. M. Smith, *Chem. Eng. Sci.*, **17**, 825 (1962).

Manuscript received August 23, 1963; revision received November 22, 1963; paper accepted November 25, 1963.